



HAL
open science

Life Cycle Assessment of Magnetite Production Using Microfluidic Devices: Moving from the Laboratory to Industrial Scale

Olga Fuentes, Juan Cruz, Emmanuel Mignard, Guido Sonnemann, Johann Osma

► **To cite this version:**

Olga Fuentes, Juan Cruz, Emmanuel Mignard, Guido Sonnemann, Johann Osma. Life Cycle Assessment of Magnetite Production Using Microfluidic Devices: Moving from the Laboratory to Industrial Scale. ACS Sustainable Chemistry & Engineering, 2023, 11 (18), pp.6932-6943. 10.1021/acssuschemeng.2c06875 . hal-04107325

HAL Id: hal-04107325

<https://cnrs.hal.science/hal-04107325v1>

Submitted on 20 Nov 2023

HAL is a multi-disciplinary open access archive for the deposit and dissemination of scientific research documents, whether they are published or not. The documents may come from teaching and research institutions in France or abroad, or from public or private research centers.

L'archive ouverte pluridisciplinaire **HAL**, est destinée au dépôt et à la diffusion de documents scientifiques de niveau recherche, publiés ou non, émanant des établissements d'enseignement et de recherche français ou étrangers, des laboratoires publics ou privés.



Distributed under a Creative Commons Attribution 4.0 International License

Life Cycle Assessment of Magnetite Production Using Microfluidic Devices: Moving from the Laboratory to Industrial Scale

Olga P. Fuentes, Juan C. Cruz, Emmanuel Mignard, Guido Sonnemann,* and Johann F. Osma*

Cite This: *ACS Sustainable Chem. Eng.* 2023, 11, 6932–6943

Read Online

ACCESS |



Metrics & More



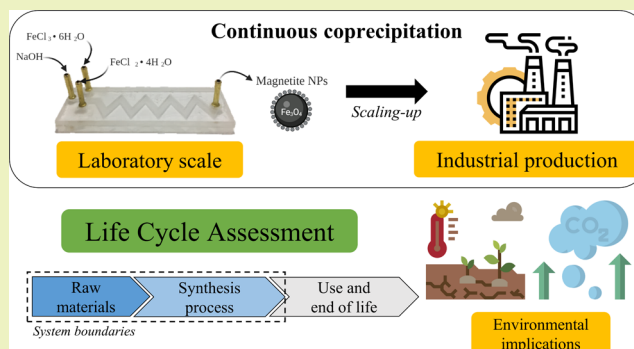
Article Recommendations



Supporting Information

ABSTRACT: Magnetite nanoparticles (MNPs) have important applications in several industrial and scientific fields for the remediation of contaminated soil and water, for instance. Emerging technologies such as microfluidic techniques have been adapted to continuously synthesize MNPs showing appealing results, such as a narrower size distribution. Therefore, this approach might become important for producing MNPs to meet industrial requirements. In this study, a life cycle assessment (LCA) is conducted to analyze and evaluate the impacts of the synthesis of MNPs performed in microfluidic devices. This LCA considers all of the steps required for MNP production at a laboratory and possible industrial scales. The LCA results showed that the rivets suitable for device inlets and outlets and the chemicals required for the synthesis process have the highest contribution to all impact categories, i.e., 80 and 90%, respectively. These results thus contribute to determining the overall environmental performance of each step during the synthesis of MNPs. The contribution analysis reveals that the manufacturing stage has a contribution of 97% at the lab scale, while the operation stage shows a contribution of 82% at the industrial scale. Finally, a sensitivity analysis is performed to identify the possible scenarios for replacing rivets required to manufacture microfluidic devices.

KEYWORDS: *life cycle assessment, magnetic nanoparticle, microfluidic, scaling-up, emerging technologies*



INTRODUCTION

Magnetite nanoparticles (MNPs) are widely used for industrial and scientific applications due to their unique electric and magnetic properties, ease of synthesis and functionalization, and feasibility for size control and polydispersity by fine-tuning synthesis parameters.¹ Some of such properties include superconductivity, superparamagnetism, water relaxation, magnetic sensitivity, etc.^{2,3} For this reason, MNPs have found meaningful applications, including the production of printed electronics, the remediation of soil and surface and groundwater, the production of drug delivery vehicles, the development of medical diagnostics devices, and the manufacturing of memory data storage devices.^{4–6} Considering that the large-scale manufacturing of MNPs is critical to enable these applications, it becomes critically important to determine which types of impacts such processes have where on the environment, covering aspects of human health, ecosystem degradation, and resource use.

MNPs can be produced by different processes based on physical, chemical, and biological methods with different mechanisms, inputs, yields, and reaction conditions.⁷ In this regard, some of the simplest and most common methods to produce MNPs include sol–gel approaches and chemical coprecipitation of iron chlorides.⁸ Alternatively, less popular

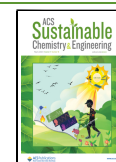
methods, due to their high associated cost and complexity, include those based on sonochemistry and thermal decomposition.^{9–11} More recently, the synthesis enabled by microfluidic devices has gained significant attention as they provide a powerful platform to prepare, functionalize, and manipulate nano/micromaterials such as magnetite.^{12–14}

Microfluidic techniques have shown advantages in nanoparticle synthesis processes that involve diffusion, emulsification, and mixing in continuous synthesis schemes.^{15–17} However, one of the main drawbacks of microfluidics is the need for sophisticated cleanroom microfabrication techniques to precisely control the device's characteristics.¹⁸ We overcame this major issue by introducing a low-cost manufacturing method for the devices that rely on widely available and inexpensive laser cutting techniques.^{19–21} Specifically, for the MNP synthesis, the microfluidic approach is attractive because of its high portability, the possibility of particle size control,

Received: November 16, 2022

Revised: April 10, 2023

Published: April 21, 2023



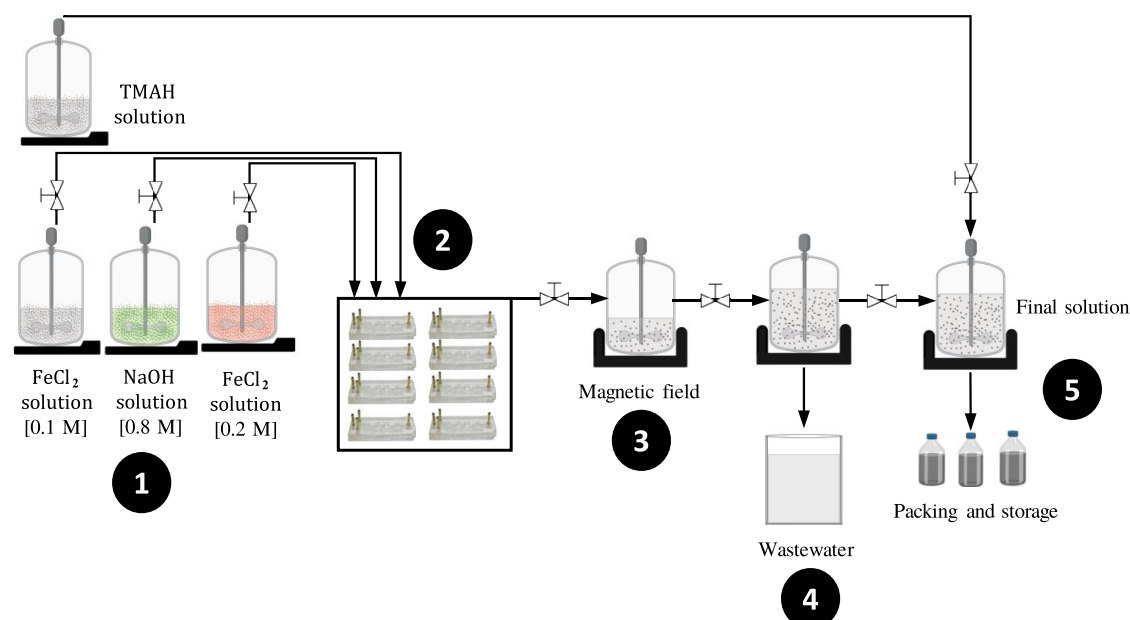


Figure 1. Operation flowchart of the MNP synthesis at an industrial scale: (1) reagent solution production, (2) synthesis of MNPs, (3) magnetic separation, (4) washing, and (5) conditioning and storage.

and applicability on a large scale.²² Also, superior control on thermal and mass transfer during nanoparticle synthesis leads to high surface-to-volume ratios and improved magnetic properties.²³ This makes such an approach an appealing route to achieve the high reproducibility required for large-scale production. However, the scaling-up of emerging technologies from the laboratory to the industrial scale involves various challenges, including adaptability to other materials, complex manufacturing and operating processes, and determining their environmental impact.²⁴ Several studies have demonstrated that there is an avenue to evaluate their environmental performance through the life cycle assessment (LCA) methodology.^{25,26}

The LCA methodology has been widely used to assess the environmental sustainability of new products and emerging technologies in the early stages.²⁷ In particular, this methodology has been used in different fields that involve nanomaterials such as photovoltaic systems,²⁸ soil remediation,²⁹ water remediation,³⁰ lithium-ion batteries using silicon nanotubes for electric vehicles,³¹ and biogas production.³² These studies have demonstrated the important role of LCA in the identification of environmental hotspots from early development phases to promote improvement actions. Therefore, this study assesses the environmental impacts related to the production of MNPs going from the laboratory scale to an industrial scale through an LCA analysis.

This work proposes a possible scaling-up of the synthesis of MNPs using many microfluidic devices working in parallel. Such an increase is envisaged to go from a laboratory scale to an industrial scale. In this context, our work aims at investigating what would be the environmental impacts of such an increase in scale and understanding the possible shifting of burdens among environmental impact categories and from one part of the product life cycle to another. Overall, the goal is to identify the portions of the process chain that contribute most to the environmental impacts as the basis for coming up with alternatives to reduce the environmental hotspots. Therefore, we carried out an LCA study considering

all of the steps related to the microfabrication of the devices and to the production of MNPs at both the laboratory and industrial scales, including materials, electricity, and wastewater generated.

METHODS

Synthesis of Magnetite Nanoparticles (MNPs). MNPs were synthesized by the continuous coprecipitation technique within a microfluidic device equipped with two inlets, as described by Florez et al.'s study.²² Briefly, the reaction is carried out by injecting through one inlet a sodium hydroxide (NaOH) solution (800 mM) at a rate of 1 mL/min and through the other a mixture of aqueous solutions of iron (II) chloride tetrahydrate ($\text{FeCl}_2 \cdot 4\text{H}_2\text{O}$) (100 mM) and iron (III) chloride hexahydrate ($\text{FeCl}_3 \cdot 6\text{H}_2\text{O}$) (200 mM) at a rate of 0.5 mL/min. Finally, the obtained MNPs were kept in an aqueous solution of tetramethylammonium hydroxide (TMAH) (2% v/v) overnight to avoid agglomeration.

Microfluidic devices were manufactured following the design for the 3D micromixer (3DB) reported by Florez et al.,²⁷ which achieved an important dynamic mixing due to its 90° elbows allowing for abrupt changes in the fluid direction. This microfabrication involves laser cutting and engraving of the microfluidic channels on poly(methyl methacrylate) (PMMA) sheets. Ethanol (96% v/v) was spread on the layers, and the surfaces were then assembled with the aid of a custom-made press that allowed for increasing the temperature. Finally, the connection to the external fluidic circuit was enabled by rivets glued to the inlets and outlets of the device.

Here, in this work, we divided this synthesis process into two different stages: (i) a manufacturing stage involving the fabrication of microfluidic devices and (ii) an operation stage including all of the processes for the synthesis of the MNPs, as described above.

Scaling-Up of the Process. The microfluidic process for the synthesis of MNPs was scaled up from the laboratory to the industrial scenario by considering production of 100 t/a. We assumed that the industrial plant based on microfluidic devices would work 100% of the time per year and that, as a first approximation, one defective device must be replaced every 2 days, i.e., $365.25/2 = 183$ devices. As the production of a single microfluidic device is 1 g/h, this implies that industrial production requires a parallel operation of $100/(1.10^{-6} \times 24 \times 365.25) + 183 = 11\,591$ microfluidic devices, as well as several pieces of industrial equipment, as shown in Figure 1. This scaling-up approach followed the framework reported by Piccinno et al.,³³ and all

stages and mass and energy balances were derived from the operation at the laboratory scale.

The MNP production process is carried out in five different stages: (1) All of the reagent solutions, i.e., FeCl₂, FeCl₃, NaOH, and TMAH solutions, should be prepared using mixing tanks and platform scales are required to measure the required reagents. Deionized water is necessary to make these solutions and is supplied through pumps from the main water tank. (2) These solutions should be pumped to each inlet of all microfluidic devices to enable the continuous synthesis of the MNPs. (3) MNP separation is assumed to be performed with the aid of a magnetic field externally applied to the collecting vessels. (4) These MNPs are washed several times with water, generating wastewater. Finally, (5) MNPs are mixed with the TMAH solution to avoid agglomeration during their storage.

The needed reagents were estimated by linearly scaling-up the process with the aid of stoichiometric ratios. Solutions of such reagents are produced using 1000 L mixing tanks. These tanks require a specific stirring energy input, which was calculated considering the density of each solution and the mixing time. Electricity consumption for pumping was calculated considering the flow rate (L/min) of each solution in the mixing tanks. Its power consumption was also calculated by taking into account power and operating time, similar to other pieces of equipment such as the laser cutter, conveyor belt, and platform scale. The pieces of equipment needed to produce MNPs at an industrial scale are summarized in Table 1. The total electricity consumption for such equipment needs is estimated at 81 233 kWh. This electricity consumption is analyzed with different electricity mixes.

Table 1. Power Consumption of the Equipment for the Production of MNPs at the Industrial Scale

equipment	power (kW)	quantity	total consumption (kWh)
laser cutter	1.5	3	4278
conveyor belt	1.12	2	12
oven	7	1	43
platform scale	0.01	7	168
mixing tank	0.5	15	1850
pump	0.37	27	74 880

Life Cycle Assessment. This study follows the LCA methodology defined in the ISO 14040-44 standard, where four steps are addressed to assess the environmental impacts of the MNP synthesis process using microfluidic devices.³⁴ These steps are (1) goal and scope definition, which includes objectives, the functional units for both scales of production, and the system boundaries; (2) life cycle inventory (LCI), which includes the collection of data related to each step in the synthesis process, determining the relevant flow of raw materials, energy, water, and waste generated; (3) life cycle impact assessment (LCIA), which classifies the inventory data according to their potential impact categories; and (4) interpretation, where the results are analyzed in terms of contributions, identification of environmental hotspots, sensitivity analysis, and alternatives for reducing the negative effects on the overall environmental performance.

Goal and Scope. This study aims to analyze and evaluate the environmental impacts associated with the synthesis process of MNPs using the 3DB micromixing device. Both manufacturing and operation stages were first addressed, on the one hand, at the laboratory scale and, on the other hand, at the industrial scale, where the increase in the production scale was achieved by increasing the number of microfluidic devices required for synthesis. One of the objectives of this work was to identify the stage and the associated subprocesses that contribute the most to the environmental impacts (which are not necessarily the same step or subprocesses according to the scales studied) and to provide possible ways for mitigating them. The function of the system was defined according to the synthesis process of MNPs for each scale. In this regard, at the laboratory scale, the functional unit was defined as 1 g/h of MNPs, while it was 100 tons

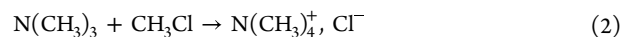
per year at the industrial scale. The LCA considered here for both scales was based on an attributional approach or descriptive "cradle-to-gate." Figure 2 shows the flowchart diagram for the synthesis of MNPs, including raw materials, the energy required, and generated waste. Additionally, the system boundaries were defined from the production of chemicals, electricity, transport, and the materials required to manufacture the microfluidic devices up to the MNP production. We excluded the final use of MNPs and their end of life as well as the production of process equipment such as mixing tanks, pumps, platform scale, and the pipeline for the industrial scale.

Life Cycle Inventory. At the laboratory scale, the life cycle inventory (LCI) was calculated based on our previous analysis of the MNP synthesis by micromixers.²² In contrast, at the industrial scale, the inventory was calculated following the scaling-up procedure reported by Piccino et al.³³ Their study proposes that scaling-up of chemical processes can be conducted from available laboratory experiments following a five-step procedure. First, we obtained all of the process stages and involved mass and energy balances for the synthesis of MNPs from our previous experiments. Second, we sketched the flow diagram with this information, as shown in Figure 2. Third, each process was scaled up according to the framework for raw materials and pieces of equipment. Fourth, the inputs and outputs of each process were scaled up. Finally, we conducted the LCA analysis of the scaled-up process.

In this study, the complete inventory was modeled in OpenLCA 1.11 software. Background data for chemicals, materials, transport, and electricity required for each stage were obtained from the Ecoinvent 3.5 database and are summarized in Tables 2 and S-1.

Transport was included at both laboratory and industrial scales to complete the inventory, considering that the MNPs are produced in Bogotá, Colombia. The distance for transporting the chemicals at the laboratory scale was assumed to be 40 km, which corresponds to the distance from a local chemical store (where the chemicals were purchased) to the laboratory. At the industrial scale, we considered that raw materials need to be imported from Qingdao, China to Bogotá, Colombia. Hence, the transport distance was assumed to be 16 882 km by ship and 1045 km by lorry from the seaport to Bogotá.

TMAH Calculation. A special case was to build the life cycle inventory of the production of TMAH that was modeled as a product system using OpenLCA software and the Ecoinvent 3.5 database. According to eq 1, TMAH is obtained from an equimolar reaction of TMACl with KOH, generating KCl as a byproduct. Moreover, TMACl is also obtained from the equimolar reaction of trimethylamine with methyl chloride, as shown in eq 2. As these production processes were reported in the database, the environmental impacts of the production of TMAH can be estimated according to the inventory reported in the Supporting information, Table S-2.



An economic allocation was considered that includes the selling price of TMAH and KCl as chemical reaction products. According to Ardente et al.,³⁵ economic allocation is suitable when the main product has a higher price than other coproducts, and therefore, the price can be related to quality features that cannot simply be measured by physical criteria. At the time of writing this article, the selling prices for TMAH (CAS: 10424-65-4) and KCl (CAS: 7447-40-7) are 1371.61 and 129.32 USD/kg, respectively.^{36,37} Thus, the allocation was defined in OpenLCA as 0.09 for KCl and 0.91 for TMAH.

Life Cycle Impact Assessment (LCIA). The impact assessment method applied in this study was the ReCiPe 2016 Midpoint (H). This method provides a higher degree of detail for measuring the environmental performance of a product or a process through the characterization factors that are representative on the global scale.^{38,39} Moreover, the ReCiPe method allowed us to determine the inventory to evaluate the land, air, and water environmental impacts and the resource scarcity associated with MNP production using a set of impact categories. Results were assessed in 18 different midpoint

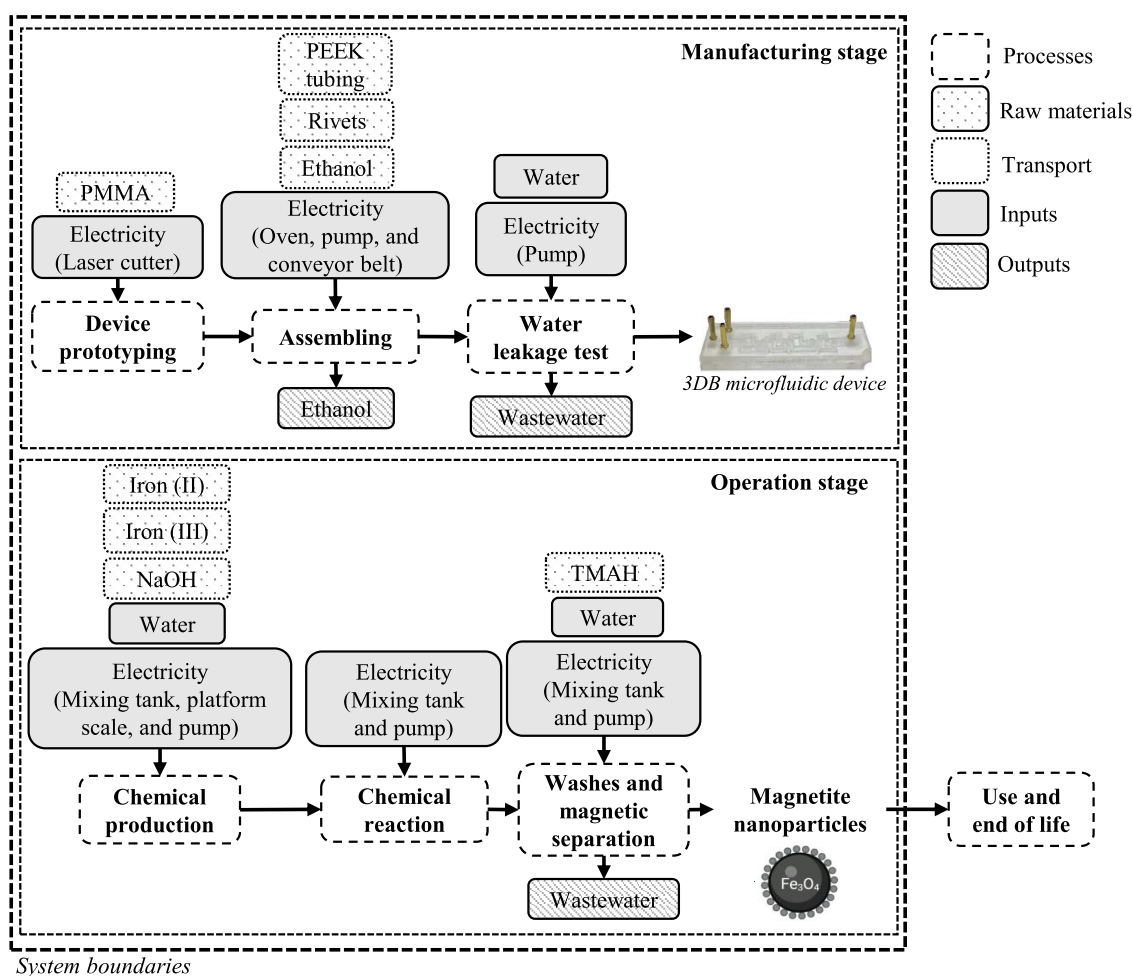


Figure 2. System boundaries for producing MNPs, considering the manufacturing and operation stages.

Table 2. Life Cycle Inventory Data for the Synthesis of MNPs at Laboratory and Industrial Scales

stage	flow	magnitude	laboratory scale 1 g/h			industrial scale 100 t/a		
			amount	unit	GSD	amount	unit	GSD
manufacturing	PMMA	volume	1.69×10^{-05}	m ³	1.10	1.93×10^{-01}	m ³	1.51
	PEEK and FEP tubing	mass				120.47	kg	1.77
	rivets	mass	4×10^{-02}	kg	1.03	456.32	kg	1.06
	ethanol	volume	2.10×10^{-05}	m ³	1.05	4.68×10^{-01}	m ³	1.51
	electricity	energy	4.73×10^{-01}	kWh	1.23	4338	kWh	1.25
	water consumption	volume	5.30×10^{-05}	m ³	1.03	2.05×10^{-01}	m ³	1.51
	transport, lorry	mass × distance	3.06	kg·km	1.23	1225.8	t·km	1.23
	transport, ship	mass × distance	1294.41	kg·km	1.23	20 497.3	t·km	1.23
	operation	iron(II) chloride tetrahydrate (FeCl ₂ ·4H ₂ O)	mass	8.60×10^{-04}	kg	1.03	85 866.8	kg
iron(III) chloride hexahydrate (FeCl ₃ ·6H ₂ O)		mass	2.33×10^{-03}	kg	1.03	233 487.2	kg	1.51
sodium hydroxide (NaOH)		mass	1.38×10^{-03}	kg	1.03	138 198.9	kg	1.51
tetramethylammonium hydroxide (TMAH)		mass	2.24×10^{-05}	kg	1.10	2240	kg	1.51
electricity		energy	7.70×10^{-02}	kWh	1.23	76 895	kWh	1.25
deionized water		volume	1.02×10^{-03}	m ³	1.03	17 045.9	m ³	1.51
transport, lorry		mass × distance	1.84×10^{-01}	kg·km	1.23	480 483.7	t·km	1.23
transport, ship		mass × distance	77.53	kg·km	1.23	778 784.5	t·km	1.23

categories, such as fine particulate matter formation (FPMF), fossil resource scarcity (FRS), freshwater ecotoxicity (FE), freshwater eutrophication (FEut), global warming (GW), human carcinogenic toxicity (HCT), human noncarcinogenic toxicity (HNCT), ionizing radiation (IR), land use (LU), marine ecotoxicity (ME), marine eutrophication (MEP), mineral resource scarcity (MRS), ozone formation, human health (OFHH), ozone formation, terrestrial

ecosystems (OFTE), stratospheric ozone depletion (SOD), terrestrial acidification (TA), terrestrial ecotoxicity (TE), and water consumption (WC). The shifting of burdens among environmental impact categories means the transfer of hotspots from one environmental impact category, for instance, CC to FEut (as often observed in the case of biosourcing chemical ingredients due to the runoff of excess fertilizer used).

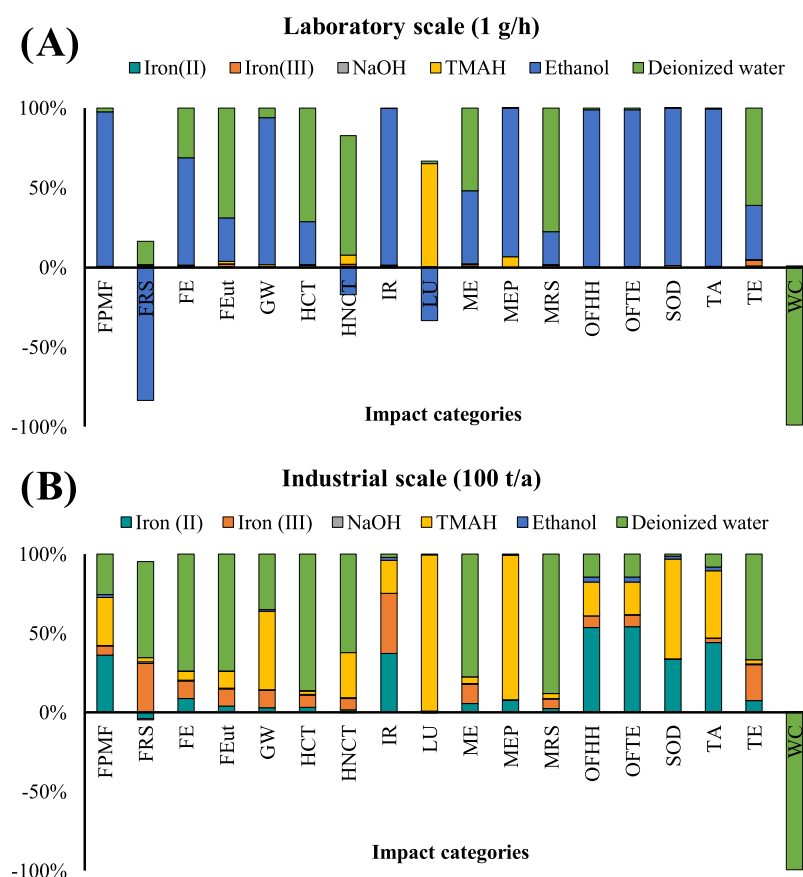


Figure 3. Contribution analysis for inputs to the generated wastewater during the synthesis of MNPs: (A) at the laboratory scale and (B) at the industrial scale.

RESULTS AND DISCUSSION

Wastewater Calculation. Wastewater generated during the synthesis of MNPs was calculated with the aid of the Wastewater Life Cycle Inventory Initiative (WW_LCI_V4.0) tool with parameters obtained from US EPI SUITE, Simple-Treat, and SimaPro software V9.0. (Ecoinvent 3.5 database and ReCiPe 2016 method).⁴⁰ SimaPro software was employed to obtain the environmental impacts of each compound present in wastewater by considering a plant located in France with a standard treatment method (see the Supporting information, Table S-3).

This approach considered some assumptions for molecules that have not been reported in the wastewater treatment tool. For example, the iron present in iron chloride(II) and iron chloride(III) was assumed to be the same iron reported in the wastewater tool. Moreover, the chlorine present in iron chloride(II) and iron chloride(III) and sodium hydroxide were assumed to be sodium chloride. Additionally, *N,N*-dimethylformamide was chosen as a good proxy of TMAH, and impacts on water treatment were taken from unpolluted wastewater reported in the Ecoinvent 3.5 database.

The relative contribution of each of these molecules to wastewater was calculated from the concentrations used in laboratory experiments; i.e., 15% iron(II), 15% iron(III), 95% NaOH, 95% TMAH, 100% ethanol, and 80% water were contributing to the wastewater. According to these results, the total impacts of the wastewater generated in the synthesis process of MNPs were estimated and are shown in Figure 3.

Figure 3A shows that ethanol, which is required to assemble the microfluidic device in the manufacturing stage, has the highest contribution to the wastewater at the laboratory scale. Ethanol has indeed the highest contribution to the following impact categories: terrestrial acidification (99%), stratospheric ozone depletion (99%), ozone formation (99%), ionizing radiation (98%), fine particulate matter formation (97%), and marine eutrophication (93%). The impacts on categories related to aquatic and terrestrial ecosystems can be attributed to emissions during the distillation process of ethanol.^{41,42}

Water consumption has the highest contribution to wastewater at the industrial scale, as shown in Figure 3B. The results show that the impacts associated with the consumption of water are dominant in nine impact categories, mainly in resource scarcity and freshwater categories. This is important because, as has already been reported, freshwater resources are of great importance within socio-economic and ecological systems as their management is key for maintaining ecological functions and biodiversity.⁴³ Moreover, inappropriate management might lead to alterations in the water cycle and the drying up of rivers, streams, and lands.⁴⁴

The TMAH molecule has a significant impact on the land use and marine eutrophication categories. These impacts are related to the high risk of exposure and the release of TMAH into the environment.⁴⁵ Moreover, this chemical is not only toxic to aquatic organisms but also harmful to human health. Several studies have indeed reported many acute and adverse effects of TMAH on human health, such as chemical burns, respiratory failure, and sudden death.⁴⁶ Accordingly, it is

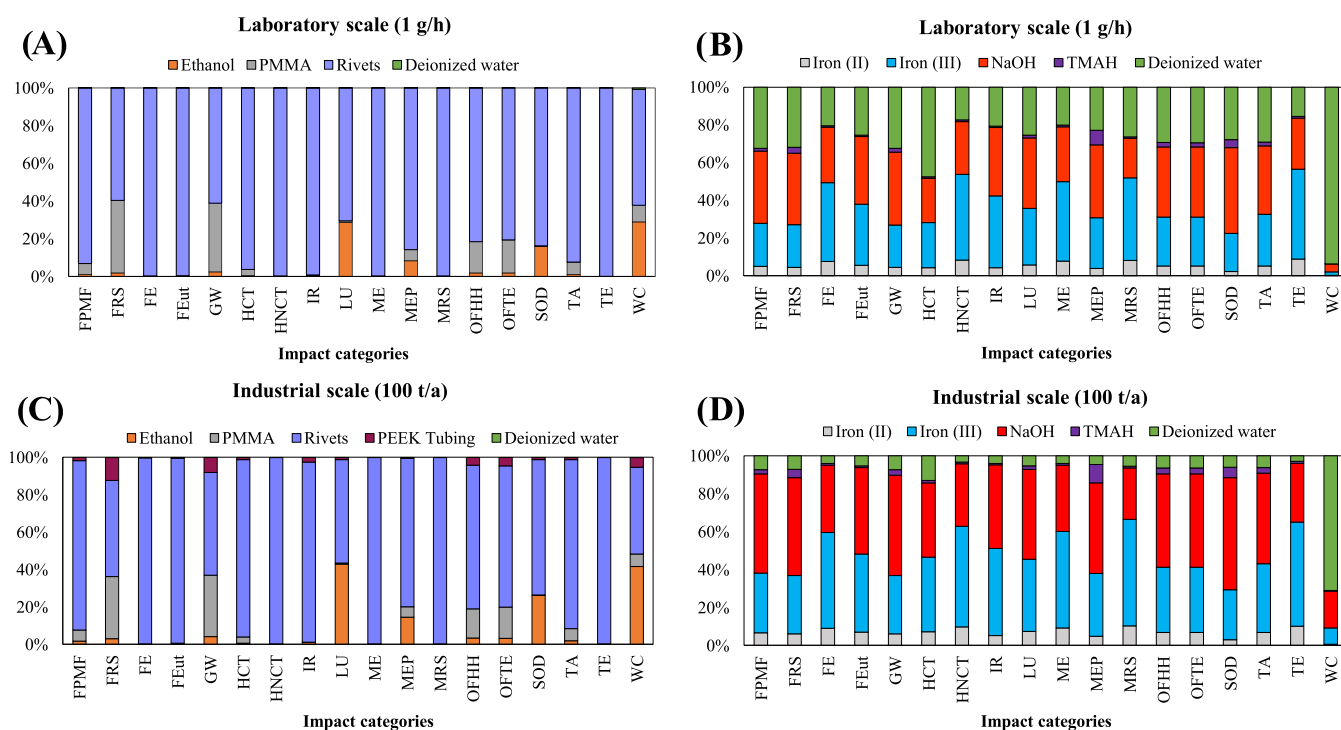


Figure 4. Environmental hotspot analysis of chemicals used for the synthesis of MNPs: at the laboratory scale: (A) manufacturing stage and (B) operation stage; and at the industrial scale: (C) manufacturing stage and (D) operation stage.

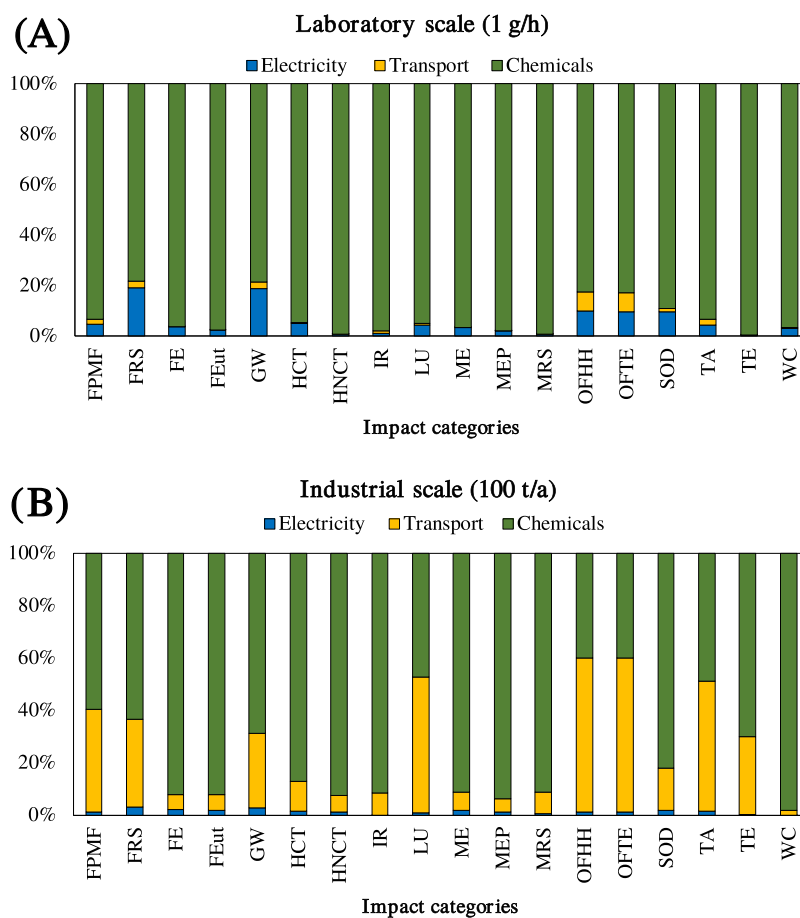


Figure 5. Contribution analysis for electricity, transport, and chemicals used to synthesize MNPs: (A) at the laboratory scale and (B) at the industrial scale.

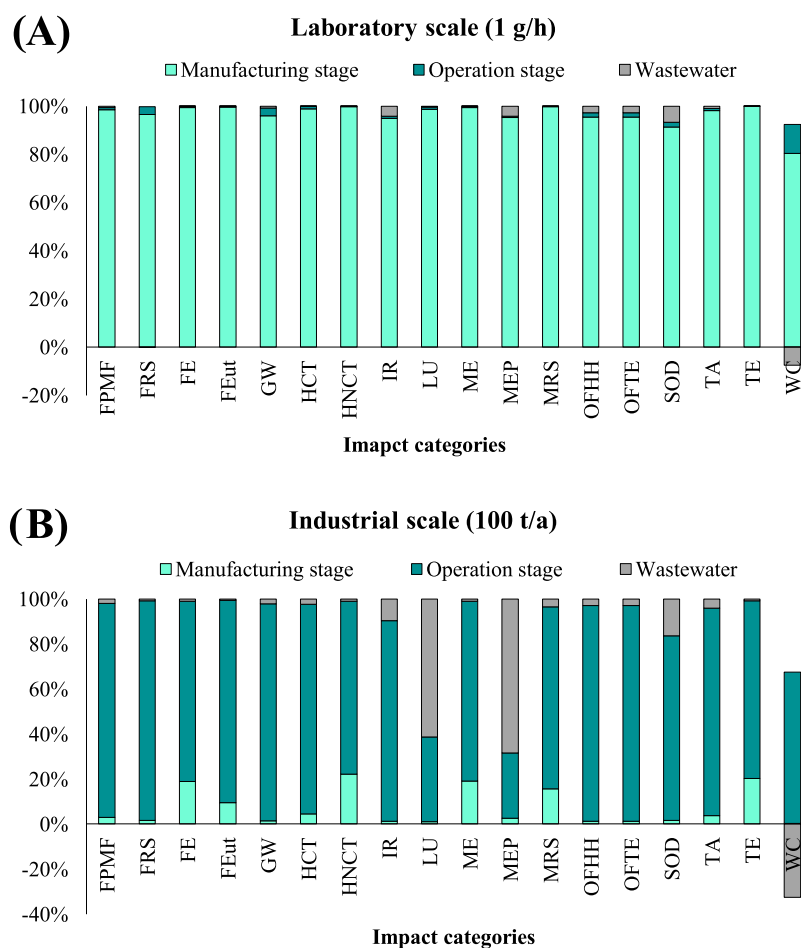


Figure 6. Total contribution of each impact for the manufacturing stage, operation stage, and wastewater at (A) laboratory scale and (B) industrial scale.

imperative to propose strategies to handle wastewater from industrial MNP synthesis.

As well known, the intensive use of nanomaterials that are synthesized through non-eco-friendly technologies may lead to the unmanaged release of toxic compounds. Considering the importance of wastewater discharges, several studies have revealed strategies to reduce toxic effects from nanomaterials synthesis that directly affect both human health and the environment. Alternatives to traditional techniques for the reuse and recycling of nanoparticles have been discussed, which involve centrifugation and solvent evaporation.⁴⁷ Recent studies have demonstrated that the use of eco-friendly routes during the production of nanoparticles is necessary to neutralize the nanoparticle waste before disposal.⁴⁸ Green alternatives to produce MNPs based on the benefits of microbes use such as bacteria, microalgae, yeast, actinomycetes, and fungi have also been reported to carry out responsible industrial production.⁴⁹

Contribution Analysis. Figure 4 provides the hotspot analysis for the synthesis of MNPs at laboratory and industrial scales. The analysis shows the magnitude of impacts for each impact category resulting from the inputs to the process.

Overall, rivets have the highest contribution for the manufacturing stage compared to other materials, approximately 80% of all impact categories. Rivets are manufactured with a brass alloy composed primarily of copper and zinc. Although this material is widely used for industrial

applications, its use involves high environmental impact, which can be attributed to properties such as corrosion resistance, absence of magnetism, and machinability.⁵⁰ Previous studies have reported that brass directly affects marine organisms, which is evidenced by the high levels of impact categories such as freshwater ecotoxicity (FE), freshwater eutrophication (FEut), and marine ecotoxicity (ME).⁵¹

In the operation stage, iron chloride(III) and NaOH contribute the most to the impact share, with approximately 40% of the contribution. According to Patiño-Ruiz et al.,⁵² these results can be attributed to the production of chemicals that involve different anthropogenic activities. They reported that these activities lead to environmental impacts related to energy usage and disposal of industrial waste, which is commonly released into soils and water sources.

The production of MNPs at the laboratory scale results in an obvious use of fewer chemicals compared with the industrial scale. However, deionized water usage has the largest contribution to the impacts at the laboratory scale. This result may be related to a large amount of water required for washing the obtained MNPs to remove excess reagents. Consequently, the environmental impacts associated with water were higher than those of chemicals.

For both scales, results in Figure 5 show that the impacts related to chemical usage dominated nearly all impact categories and, in some cases, contributed to more than 90%

Table 3. Uncertainties for LCIA Results Related to the Synthesis of MNPs at Laboratory and Industrial Scales

Laboratory Scale 1 g/h					
impact categories	mean	geometric standard deviation	5% percentile	95% percentile	CV
FPMF	3.89×10^{-03}	1.32×10^{-04}	3.68×10^{-03}	4.11×10^{-03}	3.4%
FRS	1.95×10^{-01}	9.73×10^{-03}	1.80×10^{-01}	2.11×10^{-01}	5.0%
FE	4.48×10^{-01}	1.63×10^{-02}	4.21×10^{-01}	4.75×10^{-01}	3.6%
FEut	2.46×10^{-03}	8.96×10^{-05}	2.32×10^{-03}	2.61×10^{-03}	3.6%
GW	6.42×10^{-01}	3.13×10^{-02}	5.92×10^{-01}	6.95×10^{-01}	4.9%
HCT	1.16×10^{-01}	4.10×10^{-03}	1.10×10^{-01}	1.23×10^{-01}	3.5%
HNCT	1.64×10^{01}	6.04×10^{-01}	1.54×10^{01}	1.74×10^{01}	3.7%
IR	6.69×10^{-02}	2.40×10^{-03}	6.31×10^{-02}	7.08×10^{-02}	3.6%
LU	1.10×10^{-02}	3.41×10^{-04}	1.04×10^{-02}	1.15×10^{-02}	3.1%
ME	6.50×10^{-01}	2.37×10^{-02}	6.11×10^{-01}	6.89×10^{-01}	3.6%
MEP	1.75×10^{-04}	5.71×10^{-06}	1.66×10^{-04}	1.85×10^{-04}	3.3%
MRS	3.89×10^{-02}	1.43×10^{-03}	3.66×10^{-02}	4.13×10^{-02}	3.7%
OFHH	2.64×10^{-03}	9.62×10^{-05}	2.48×10^{-03}	2.80×10^{-03}	3.7%
OFTE	2.71×10^{-03}	9.88×10^{-05}	2.55×10^{-03}	2.87×10^{-03}	3.6%
SOD	6.96×10^{-07}	2.38×10^{-08}	6.58×10^{-07}	7.35×10^{-07}	3.4%
TA	1.13×10^{-02}	3.83×10^{-04}	1.07×10^{-02}	1.20×10^{-02}	3.4%
TE	6.55×10^{01}	2.42×10^{00}	6.16×10^{01}	6.94×10^{01}	3.7%
WC	9.00×10^{-03}	2.41×10^{-04}	8.60×10^{-03}	9.39×10^{-03}	2.7%
Industrial Scale 100 t/a					
impact categories	mean	geometric standard deviation	5% percentile	95% percentile	CV
FPMF	1.58×10^{03}	2.73×10^{02}	1.19×10^{03}	2.07×10^{03}	17.3%
FRS	1.62×10^{05}	2.90×10^{04}	1.19×10^{05}	2.15×10^{05}	17.9%
FE	2.81×10^{04}	5.91×10^{03}	1.97×10^{04}	3.92×10^{04}	21.0%
FEut	3.21×10^{02}	7.44×10^{01}	2.14×10^{02}	4.59×10^{02}	23.2%
GW	5.78×10^{05}	1.12×10^{05}	4.16×10^{05}	7.83×10^{05}	19.4%
HCT	3.12×10^{04}	6.72×10^{03}	2.12×10^{04}	4.35×10^{04}	21.5%
HNCT	8.98×10^{05}	1.85×10^{05}	6.36×10^{05}	1.25×10^{06}	20.6%
IR	6.17×10^{04}	1.60×10^{04}	3.89×10^{04}	9.07×10^{04}	25.9%
LU	5.89×10^{03}	9.67×10^{02}	4.42×10^{03}	7.66×10^{03}	16.4%
ME	4.04×10^{04}	8.39×10^{03}	2.85×10^{04}	5.60×10^{04}	20.7%
MEP	2.86×10^{01}	6.46×10^{00}	1.92×10^{01}	4.07×10^{01}	22.6%
MRS	2.94×10^{03}	6.46×10^{02}	2.04×10^{03}	4.18×10^{03}	22.0%
OFHH	2.66×10^{03}	3.83×10^{02}	2.10×10^{03}	3.35×10^{03}	14.4%
OFTE	2.69×10^{03}	3.87×10^{02}	2.12×10^{03}	3.38×10^{03}	14.4%
SOD	4.75×10^{-01}	1.11×10^{-01}	3.15×10^{-01}	6.85×10^{-01}	23.4%
TA	3.62×10^{03}	5.53×10^{02}	2.81×10^{03}	4.61×10^{03}	15.3%
TE	3.89×10^{06}	6.24×10^{05}	2.98×10^{06}	5.01×10^{06}	16.0%
WC	2.80×10^{04}	9.11×10^{03}	1.63×10^{04}	4.57×10^{04}	32.5%

of life cycle burdens. At the industrial scale, this contribution distribution is applied to all impact categories except land use, ozone formation affecting human health, ozone formation affecting terrestrial ecosystems, and terrestrial acidification impact categories, where impacts due to transport are significant. The impact of transport is evidently higher at the industrial scale because more energy is needed to import the larger amount of chemicals required in that case.

Transport considered at the laboratory scale showed lower environmental implications due to the shorter distance involved. In contrast, at the industrial scale, we assumed that all chemicals were transported from China to Colombia using freight transport by ship and lorry. Consequently, transport impacted the ozone formation category significantly due to the emissions of methane and volatile organic compounds (VOC) to the atmosphere.⁵³

Figure 6 shows the total contribution of each impact for processing each stage and wastewater during the synthesis process of MNPs. The manufacturing stage at the laboratory scale shows the most considerable contribution, with

approximately 97% of all impact categories. As mentioned above, these results are attributed to rivet usage to assemble the microfluidic device's inlets and outlets and the use of chemicals such as iron chloride(II) and sodium hydroxide.

The operation stage has the highest contribution to the 16 impact categories analyzed at the industrial scale. This stage is mainly affected by the intensive use of chemicals for the synthesis process and their transport. On the other hand, wastewater generates significantly higher impacts than the two other stages in the land use and marine eutrophication categories. Wastewater contributes to 65% of considered categories, which can be mainly attributed to TMAH usage (see Figure 3B).

Alternatives to Reduce the Environmental Hotspots.

The environmental hotspot analysis revealed that rivets have the largest contribution to all impact categories at both laboratory and industrial scales. Therefore, their possible replacement with another type of fitting made of a more sustainable material might be appealing as an eco-design strategy. In this regard, polyether ketone (PEEK) fittings could

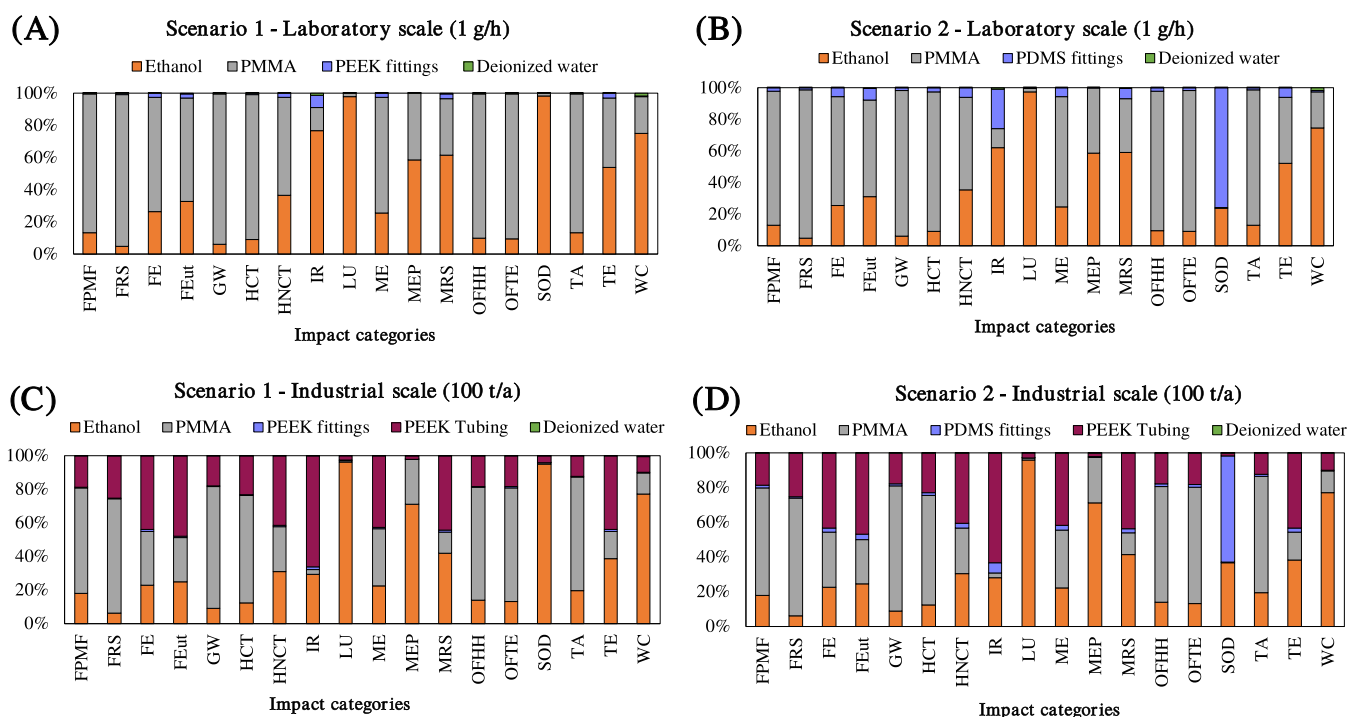


Figure 7. Sensitivity analysis for the two alternatives considered to replace rivets: (A) scenario 1 at the laboratory scale, (B) scenario 2 at the laboratory scale, (C) scenario 1 at the industrial scale, and (D) scenario 2 at the industrial scale.

be a promising alternative, as evidenced by their relatively low impact compared with other materials when considered for the pipeline in our process at the industrial scale (see Figure 4). Similarly, other fittings such as PDMS connectors, which have been widely used for prototyping microfluidic chips, might be an alternative to replace the rivets.^{54,55}

Another alternative to reduce the impacts of global warming and fossil resource scarcity categories related to the manufacturing stage is to decrease the thickness of the PMMA sheets. Indeed, 3 mm PMMA sheets were used in the work of Florez et al.,²² and the use of 1 mm acrylic sheets would reduce the impacts related to these categories by one-third. Alternatively, one can reduce the amount of ethanol while manufacturing microfluidic devices.

A third strategy is related to mitigating the high contribution of NaOH (above 40%) to the impacts associated with the chemicals used in most categories along the operation stage. This reagent is used to adjust the pH during the MNP synthesis. Sodium carbonate can be used alternatively for pH adjustment since it has already been tested experimentally for that purpose with fewer environmental effects.⁵² Alternatively, one can also reduce the amount of deionized water to wash the MNPs.

Finally, after the production of MNPs, TMAH is used to stabilize them in suspension by avoiding agglomeration during the storage and packaging stages. Although TMAH has been reported as a hazardous chemical, the associated impact is not higher than that of other chemicals, with a contribution of only about 2%. Therefore, replacing this compound would not necessarily translate into enhanced environmental performance.

Uncertainty and Sensitivity Analysis. In this study, an uncertainty analysis was performed to determine the reliability of the results. Monte Carlo simulations were performed with 1000 iterations at the 95% confidence interval using OpenLCA

v1.11.0 to estimate the uncertainties of LCIA results. Inventory data sources were assessed using the Pedigree matrix approach, and then log-normal distributions were defined based on the calculated geometric standard deviation (GSD).⁵⁶ The results of the Monte Carlo simulation are summarized in Table 3, which includes information on the uncertainty for impact results in terms of the mean, GSD, 5 and 95% percentiles, and the coefficient of variation (CV). The last is the ratio between the GSD and the mean, which indicates the variation of the uncertainty of the impact category results.^{57,58} Results revealed that the CV for the laboratory scale was lower than that for the industrial scale. These findings were expected due to the uncertainty of the inventory data since the inventory was acquired from experimental measurements for the laboratory scale, whereas inventory data were mostly estimated for the industrial scale. Moreover, the synthesis of MNPs using emerging technologies such as microfluidics involves several assumptions, leading to a large degree of uncertainty in the impact scores.

A sensitivity analysis was performed considering the environmental hotspot analysis. Results demonstrated that rivet usage directly affects the manufacturing of microfluidic devices. Therefore, the sensitivity analysis included two alternatives as a replacement for rivets. The PEEK fittings were represented by scenario 1, and the PDMS fittings were represented by scenario 2. Figure 7 shows each scenario's environmental performance in terms of its contribution to the manufacturing process. At both the laboratory and industrial scales, PEEK fittings contributed 0.06 and 0.05% to each impact category, respectively. The contribution from scenario 2 was 2.6% at the laboratory scale and 2.3% at the industrial scale, respectively. Therefore, scenario 1 might be the best alternative for replacing rivets because it might reduce environmental burdens by around ~99.9% compared to the use of rivets.

Additionally, we carried out a supplementary sensitivity analysis to investigate the influence of the geographical electricity mix on the environmental implications of magnetite nanoparticle (MNP) production at an industrial scale. We compared the electricity mixes of Colombia, France, China, Russia, and the United States to assess their respective environmental impacts. The findings revealed a notable increase in carbon-intensive electricity mixes, specifically those of Russia, China, and the United States, which demonstrated the highest contribution (refer to the Supporting Information, Tables S-4 and S-5).

The electricity analysis indicated that the French electricity grid contributed the least to the majority of impact categories. Similarly, the Colombian grid exhibited the second-lowest contribution to the overall impact.

CONCLUSIONS

This work reports on a detailed LCA study to evaluate the environmental impacts of producing MNPs using microfluidic devices. The LCA was performed by employing inventory data obtained from laboratory experiments and scaling-up calculations as well as the uncertainties related to the input data. The environmental hotspot analysis of chemicals revealed that rivets to connect the microfluidic devices to tubing had the highest contribution to the manufacturing stage, reaching about 80% of all evaluated impact categories. Based on the sensitivity analysis, it can be concluded that it is possible to reduce environmental impacts by changing the rivets for PEEK fittings. Moreover, other alternatives could be considered, such as reducing the thickness of the PMMA sheets and replacing NaOH with a more environmentally friendly base.

In this regard, this work reports on the first LCA study of microfluidic devices, which we are aware of, that consider scaling-up calculations. Furthermore, the industrial production of the MNPs introduced here is an innovative process whose environmental impact, to our knowledge, had not been analyzed previously. Therefore, this study contributes to studying this process' overall feasibility by providing detailed information on the implementation of the LCA methodology to assess comprehensively emerging technologies such as microfluidics. This work represents a holistic understanding of the potential environmental impacts of MNP synthesis processes. Moreover, it paves the way for further analysis of the overall sustainability and eventual introduction of such emerging technologies into well-established manufacturing processes. Finally, this work is expected to help future environmental impact studies of nanomaterial production at the laboratory and industrial scales.

ASSOCIATED CONTENT

Supporting Information

The Supporting Information is available free of charge at <https://pubs.acs.org/doi/10.1021/acssuschemeng.2c06875>.

Ecoinvent data sets used for the production of MNPs, data related to the inventory for the production of tetramethylammonium hydroxide (TMAH), impacts of molecules in the wastewater, impacts of each electricity mix on the manufacturing and operation stages at laboratory and industrial scales, and additional figures for the sensitivity analysis (PDF)

AUTHOR INFORMATION

Corresponding Authors

Guido Sonnemann – CNRS, Bordeaux INP, ISM, UMR 5255, Univ. Bordeaux, F-33400 Talence, France;

orcid.org/0000-0003-2581-1910;

Email: guido.sonnemann@u-bordeaux.fr

Johann F. Osma – Department of Electrical and Electronic Engineering, Universidad de Los Andes, 111711 Bogotá, DC, Colombia; Department of Biomedical Engineering, Universidad de Los Andes, 111711 Bogotá, DC, Colombia;

orcid.org/0000-0003-2928-3406; Email: jf.osma43@uniandes.edu.co

Authors

Olga P. Fuentes – Department of Electrical and Electronic Engineering, Universidad de Los Andes, 111711 Bogotá, DC, Colombia

Juan C. Cruz – Department of Biomedical Engineering, Universidad de Los Andes, 111711 Bogotá, DC, Colombia;

orcid.org/0000-0002-7790-7546

Emmanuel Mignard – CNRS, Bordeaux INP, ISM, UMR 5255, Univ. Bordeaux, F-33400 Talence, France;

orcid.org/0000-0003-3551-2842

Complete contact information is available at:

<https://pubs.acs.org/10.1021/acssuschemeng.2c06875>

Funding

O.P.F. was funded by the Ministerio de Ciencia, Tecnología e Innovación (Minciencias, Colombia), grant number 766 of 2016.

Notes

The authors declare no competing financial interest.

ACKNOWLEDGMENTS

The authors thank the School of Engineering at Universidad de los Andes for financially supporting this work, the University of Bordeaux, France for the academic support and facility access during the doctoral internship of O.P.F. Special thanks to Dr. Philippe Loubet for his technical support with the calculations using the wastewater tool.

REFERENCES

- (1) De Montferrand, C.; Hu, L.; Milosevic, I.; Russier, V.; Bonnin, D.; Motte, L.; Brioude, A.; Lalatonne, Y. Iron Oxide Nanoparticles with Sizes, Shapes and Compositions Resulting in Different Magnetization Signatures as Potential Labels for Multiparametric Detection. *Acta Biomater.* **2013**, *9*, 6150–6157.
- (2) Laconte, L.; Nitin, N.; Bao, G. Magnetic Nanoparticle Probes. *Mater. Today* **2005**, *8*, 32–38.
- (3) Mornet, S.; Vasseur, S.; Grasset, F.; Veverka, P.; Goglio, G.; Demourgues, A.; Portier, J.; Pollert, E.; Duguet, E. Magnetic Nanoparticle Design for Medical Applications. *Prog. Solid State Chem.* **2006**, *34*, 237–247.
- (4) Khan, I.; Saeed, K.; Khan, I. Nanoparticles: Properties, Applications and Toxicities. *Arabian J. Chem.* **2019**, *12*, 908–931.
- (5) Marimón-Bolívar, W.; González, E. E. Green Synthesis with Enhanced Magnetization and Life Cycle Assessment of Fe₃O₄ Nanoparticles. *Environ. Nanotechnol., Monit. Manage.* **2018**, *9*, 58–66.
- (6) Sadhukhan, J.; Joshi, N.; Shemfe, M.; Lloyd, J. R. Life Cycle Assessment of Sustainable Raw Material Acquisition for Functional Magnetite Bionanoparticle Production. *J. Environ. Manage.* **2017**, *199*, 116–125.
- (7) Feijoo, S.; González-García, S.; Moldes-Diz, Y.; Vazquez-Vazquez, C.; Feijoo, G.; Moreira, M. T. Comparative Life Cycle

Assessment of Different Synthesis Routes of Magnetic Nanoparticles. *J. Cleaner Prod.* **2017**, *143*, 528–538.

(8) Laurent, S.; Forge, D.; Port, M.; Robic, C.; Vander Elst, L.; Muller, R. N. Magnetic Iron Oxide Nanoparticles: Synthesis, Stabilization, Vectorization, Physicochemical Characterizations, and Biological Applications. *Chem. Rev.* **2010**, *110*, 2574.

(9) Dheyab, M. A.; Abdul, A.; Jameel, M. S. Mechanisms of Effective Gold Shell on Fe₃O₄ Core Nanoparticles Formation Using Sonochemistry Method. *Ultrason. Sonochem.* **2019**, *64*, No. 104865.

(10) Bagheri, S.; Aghaei, H.; Ghaedi, M.; Asfaram, A.; Monajemi, M.; Akbar, A. Synthesis of Nanocomposites of Iron Oxide/Gold (Fe₃O₄/Au) Loaded on Activated Carbon and Their Application in Water Treatment by Using Sonochemistry: Optimization Study. *Ultrason. Sonochem.* **2018**, *41*, 279–287.

(11) Xu, L.; Jiao, R.; Tao, X.; Yi, X.; Wei, D. One-Step Thermal Decomposition of C₄H₄ FeO₆ to Fe₃O₄@carbon Nano-Composite for High-Performance Lithium-Ion Batteries. *Mater. Chem. Phys.* **2020**, *239*, No. 122024.

(12) Luo, G.; Du, L.; Wang, Y.; Wang, K. Recent Developments in Microfluidic Device-Based Preparation, Functionalization, and Manipulation of Nano- and Micro-Materials. *Particuology* **2019**, *45*, 1–19.

(13) Luo, G.; Du, L.; Wang, Y.; Lu, Y.; Xu, J. Controllable Preparation of Particles with Microfluidics. *Particuology* **2011**, *9*, 545–558.

(14) Tomeh, M. A.; Zhao, X. Recent Advances in Microfluidics for the Preparation of Drug and Gene Delivery Systems. *Mol. Pharmaceutics* **2020**, *17*, 4421–4434.

(15) Boleininger, J.; Kurz, A.; Reuss, V.; Sönnichsen, C. Microfluidic Continuous Flow Synthesis of Rod-Shaped Gold and Silver Nanocrystals. *Phys. Chem. Chem. Phys.* **2006**, *8*, 3824–3827.

(16) Makgwane, P. R.; Ray, S. S. Synthesis of Nanomaterials by Continuous-Flow Microfluidics: A Review. *J. Nanosci. Nanotechnol.* **2014**, *14*, 1338–1363.

(17) Britton, J.; Raston, C. L. Multi-Step Continuous-Flow Synthesis. *Chem. Soc. Rev.* **2017**, *46*, 1250–1271.

(18) Faustino, V.; Catarino, S. O.; Lima, R.; Minas, G. Biomedical Microfluidic Devices by Using Low-Cost Fabrication Techniques: A Review. *J. Biomech.* **2016**, *49*, 2280–2292.

(19) Yuen, P. K.; Goral, V. N. Low-Cost Rapid Prototyping of Flexible Microfluidic Devices Using a Desktop Digital Craft Cutter. *Lab Chip* **2010**, *10*, 384–387.

(20) Nie, J.; Liang, Y.; Zhang, Y.; Le, S.; Li, D.; Zhang, S. One-Step Patterning of Hollow Microstructures in Paper by Laser Cutting to Create Microfluidic Analytical Devices. *Analyst* **2013**, *138*, 671–676.

(21) Fuentes, O. P.; Noguera, M. J.; Peñaranda, P. A.; Flores, S. L.; Cruz, J. C.; Osmá, J. F. Micromixers for Wastewater Treatment and Their Life Cycle Assessment (LCA). In *Advances in Microfluidics and Nanofluids*; Sohél Murshed, S. M., Ed.; IntechOpen, 2021; pp 1–15. DOI: 10.5772/intechopen.96822.

(22) Florez, S. L.; Campaña, A. L.; Noguera, M. J.; Quezada, V.; Fuentes, O. P.; Cruz, J. C.; Osmá, J. F. CFD Analysis and Life Cycle Assessment of Continuous Synthesis of Magnetite Nanoparticles Using 2D and 3D Micromixers. *Micromachines* **2022**, *13*, 970.

(23) Gioria, E.; Signorini, C.; Wisniewski, F.; Gutierrez, L. Green Synthesis of Time-Stable Palladium Nanoparticles Using Microfluidic Devices. *J. Environ. Chem. Eng.* **2020**, *8*, No. 104096.

(24) Cong, H.; Zhang, N. Perspectives in Translating Microfluidic Devices from Laboratory Prototyping into Scale-up Production. *Biomicrofluidics* **2022**, *16*, No. 021301.

(25) Glogic, E.; Claverie, M.; Jubayed, M.; Musumeci, V.; Carême, C.; Martin, F.; Sonnemann, G.; Aymonier, C. Greening Pathways for Synthetic Talc Production Based on the Supercritical Hydrothermal Flow Process. *ACS Sustainable Chem. Eng.* **2021**, *9*, 16597–16605.

(26) Tsang, M. P.; Philippot, G.; Aymonier, C.; Sonnemann, G. Supercritical Fluid Flow Synthesis to Support Sustainable Production of Engineered Nanomaterials: Case Study of Titanium Dioxide. *ACS Sustainable Chem. Eng.* **2018**, *6*, 5142–5151.

(27) Hischier, R. Life cycle assessment of engineered nanomaterials. In *Health and Environmental Safety of Nanomaterials*; Elsevier, 2021; pp 443–458. DOI: 10.1016/B978-0-12-820505-1.00001-8.

(28) Kim, J.; Rivera, J. L.; Meng, T. Y.; Laratte, B.; Chen, S. Review of Life Cycle Assessment of Nanomaterials in Photovoltaics. *Sol. Energy* **2016**, *133*, 249–258.

(29) Visentin, C.; Braun, A. B.; Trentin, A. W. da S.; Thomé, A. Life Cycle Assessment of Soil Remediation Using Nanomaterials. *Nanomater. Soil Remediat.* **2021**, 133–150.

(30) Bartolozzi, I.; Daddi, T.; Punta, C.; Fiorati, A.; Iraldo, F. Life Cycle Assessment of Emerging Environmental Technologies in the Early Stage of Development: A Case Study on Nanostructured Materials. *J. Ind. Ecol.* **2020**, *24*, 101–115.

(31) Deng, Y.; Ma, L.; Li, T.; Li, J.; Yuan, C. Life Cycle Assessment of Silicon-Nanotube-Based Lithium Ion Battery for Electric Vehicles. *ACS Sustainable Chem. Eng.* **2019**, *7*, 599–610.

(32) Hijazi, O.; Abdelsalam, E.; Samer, M.; Attia, Y. A.; Amer, B. M. A.; Amer, M. A.; Badr, M.; Bernhardt, H. Life Cycle Assessment of the Use of Nanomaterials in Biogas Production from Anaerobic Digestion of Manure. *Renewable Energy* **2020**, *148*, 417–424.

(33) Piccinno, F.; Hischier, R.; Seeger, S.; Som, C. From Laboratory to Industrial Scale: A Scale-up Framework for Chemical Processes in Life Cycle Assessment Studies. *J. Cleaner Prod.* **2016**, *135*, 1085–1097.

(34) ISO. ISO 14040:1997 - Environmental management - Life Cycle Assessment - Principles and Framework, International organization for standardization. <https://www.iso.org/standard/23151.html> (accessed Oct 10, 2022).

(35) Ardente, F.; Cellura, M. Economic Allocation in Life Cycle Assessment: The State of the Art and Discussion of Examples. *J. Ind. Ecol.* **2012**, *16*, 387–398.

(36) Sigma Aldrich Home Page. Tetramethylammonium hydroxide (TMAH). <https://www.sigmaaldrich.com/CO/es/product/sigma/t7505> (accessed Oct 10, 2022).

(37) Sigma Aldrich Home Page. Potassium chloride (KCl). <https://www.sigmaaldrich.com/CO/es/product/sigald/p3911> (accessed Oct 10, 2022).

(38) Huijbregts, M. A. J.; Steinmann, Z. J. N.; Elshout, P. M. F.; Stam, G.; Verones, F.; Vieira, M.; Zijp, M.; Hollander, A.; van Zelm, R. ReCiPe2016: A Harmonised Life Cycle Impact Assessment Method at Midpoint and Endpoint Level. *Int. J. Life Cycle Assess.* **2017**, *22*, 138–147.

(39) Basosi, R.; Bonciani, R.; Frosali, D.; Manfreda, G.; Parisi, M. L.; Sansone, F. Life Cycle Analysis of a Geothermal Power Plant: Comparison of the Environmental Performance with Other Renewable Energy Systems. *Sustainability* **2020**, *12*, No. 2786.

(40) Muñoz, I. *Wastewater Life Cycle Inventory Initiative. WW LCI Version 4.0: Model Documentation*; Aalborg: Denmark, 2021. <http://lca-net.com/clubs/wastewater/>.

(41) Cavalett, O.; Chagas, M. F.; Seabra, J. E. A.; Bonomi, A. Comparative LCA of Ethanol versus Gasoline in Brazil Using Different LCIA Methods. *Int. J. Life Cycle Assess.* **2013**, *18*, 647–658.

(42) Fito, J.; Tefera, N.; Kloos, H.; Van Hulle, S. W. H. Physicochemical Properties of the Sugar Industry and Ethanol Distillery Wastewater and Their Impact on the Environment. *Sugar Tech* **2019**, *21*, 265–277.

(43) Bayart, J. B.; Bulle, C.; Deschênes, L.; Margni, M.; Pfister, S.; Vince, F.; Koehler, A. A Framework for Assessing Off-Stream Freshwater Use in LCA. *Int. J. Life Cycle Assess.* **2010**, *15*, 439–453.

(44) Koehler, A. Water Use in LCA: Managing the Planet's Freshwater Resources. *Int. J. Life Cycle Assess.* **2008**, *13*, 451–455.

(45) Kim, T. K.; Lee, D.; Lee, C.; Hwang, Y. S.; Zoh, K. D. Degradation of Tetramethylammonium Hydroxide (TMAH) during UV-LED/H₂O₂ Reaction: Degassing Effect, Radical Contribution, and Degradation Mechanism. *J. Hazard. Mater.* **2022**, *440*, No. 129781.

(46) Innocenzi, V.; Zueva, S. B.; Ippolito, N. M.; Ferella, F.; Prisciandaro, M.; Vegliò, F. A Review of the Existing and Emerging Technologies for Wastewaters Containing Tetramethyl Ammonium

Hydroxide (TMAH) and Waste Management Systems in Micro-Chip Microelectronic Industries. *Chemosphere* **2022**, *307*, No. 135913.

(47) McCourt, K. M.; Cochran, J.; Abdelbasir, S. M.; Carraway, E. R.; Tzeng, T. R. J.; Tsyusko, O. V.; Vanegas, D. C. Potential Environmental and Health Implications from the Scaled-Up Production and Disposal of Nanomaterials Used in Biosensors. *Biosensors* **2022**, *12*, No. 1082.

(48) George, B.; John, A. B.; Priyanila, M.; Suchithra, T. V. Two-Faced Nanomaterials: Routes to Resolve Nanowaste. *Int. J. Environ. Sci. Technol.* **2022**, 2013.

(49) Brar, K. K.; Magdouli, S.; Othmani, A.; Ghanei, J.; Narisetty, V.; Sindhu, R.; Binod, P.; Pugazhendhi, A.; Awasthi, M. K.; Pandey, A. Green Route for Recycling of Low-Cost Waste Resources for the Biosynthesis of Nanoparticles (NPs) and Nanomaterials (NMs)-A Review. *Environ. Res.* **2022**, *207*, No. 112202.

(50) Stavroulakis, P.; Toulfatzis, A. I.; Pantazopoulos, G. A.; Paipetis, A. S. Machinable Leaded and Eco-Friendly Brass Alloys for High Performance Manufacturing Processes: A Critical Review. *Metals* **2022**, *12*, No. 246.

(51) Sclodnick, T.; Sutton, S.; Selby, T.; Dwyer, R.; Gace, L. Environmental Impacts of Brass Mesh Nets on Open Ocean Aquaculture Pens in Tropical Marine Environments. *Aquaculture* **2020**, *524*, No. 735266.

(52) Patiño-Ruiz, D. A.; Meramo-Hurtado, S. I.; González-Delgado, Á. D.; Herrera, A. Environmental Sustainability Evaluation of Iron Oxide Nanoparticles Synthesized via Green Synthesis and the Coprecipitation Method: A Comparative Life Cycle Assessment Study. *ACS Omega* **2021**, *6*, 12410–12423.

(53) Sappa, G.; Iacurto, S.; Ponzi, A.; Tatti, F.; Torretta, V.; Viotti, P. The LCA Methodology for Ceramic Tiles Production by Addition of MSWI BA. *Resources* **2019**, *8*, No. 93.

(54) Saarela, V.; Franssila, S.; Tuomikoski, S.; Marttila, S.; Östman, P.; Sikanen, T.; Kotiaho, T.; Kostianen, R. Re-Usable Multi-Inlet PDMS Fluidic Connector. *Sens. Actuators, B* **2006**, *114*, 552–557.

(55) Zhang, Q.; Gong, M. Prototyping of Poly(Dimethylsiloxane) Interfaces for Flow Gating, Reagent Mixing, and Tubing Connection in Capillary Electrophoresis. *J. Chromatogr. A* **2014**, *1324*, 231–237.

(56) Frischknecht, R.; Jungbluth, N.; Althaus, H.-J.; Doka, G.; Dones, R.; Heck, T.; Hellweg, S.; Hirschler, R.; Nemecek, T.; Rebitzer, G.; Spielmann, M.; Wernet, G. *Swiss Centre for Life Cycle Inventories A Joint Initiative of the ETH Domain and Swiss Federal Offices Overview and Methodology Data v2.0 (2007)*, 2007.

(57) Ferrari, A. M.; Volpi, L.; Pini, M.; Siligardi, C.; García-Muñia, F. E.; Settembre-Blundo, D. Building a Sustainability Benchmarking Framework of Ceramic Tiles Based on Life Cycle Sustainability Assessment (LCSA). *Resources* **2019**, *8*, No. 11.

(58) Guo, M.; Murphy, R. J. LCA Data Quality: Sensitivity and Uncertainty Analysis. *Sci. Total Environ.* **2012**, *435–436*, 230–243.

Recommended by ACS

Size and Composition Control of Magnetic Nanoparticles

Dingchen Wen, Nicholas Kirkwood, *et al.*

MAY 09, 2023

THE JOURNAL OF PHYSICAL CHEMISTRY C

READ 

Energy Transfer from Magnetic Iron Oxide Nanoparticles: Implications for Magnetic Hyperthermia

Gloria Tabacchi, Ettore Fois, *et al.*

MAY 17, 2023

ACS APPLIED NANO MATERIALS

READ 

Investigating the Use of Magnetic Nanoparticles As Alternative Sintering Agents in Selective Laser Sintering (SLS) 3D Printing of Oral Tablets

Yu Zhang, Mohammed Maniruzzaman, *et al.*

FEBRUARY 06, 2023

ACS BIOMATERIALS SCIENCE & ENGINEERING

READ 

Low-Gradient Magnetophoresis of Nanospheres and Nanorods through a Single Layer of Paper

James Kah Chun Law, JitKang Lim, *et al.*

MARCH 29, 2023

LANGMUIR

READ 

Get More Suggestions >